

# **8th Annual International RoboBoat Competition**

**2015 NCKU**

## ***Ironboat***

Advisor

***Professor Yung-Yu Chen, Gene Hou***

Authors

***You-Chen Hsiao, Wei-Ting Chen, Hao Li, Pei-Yu Chang***

Sensing and applications laboratory 611

Department of System and Naval Mechatronics Engineering,

National Cheng Kung University, Taiwan



# 1. Abstract

The Ironboat, designed by NCKU Roboat Team, was built for the purpose of entering the ONR's 8th International Roboat Competition held by AUVERSI Foundation and it is the 6th generation from the prototype of SNAME 99.

For enhancing the overall performance of this new version, we redesign it by adding pontoon and enlarging the deck area of the boat. Based on these modification, the capabilities of straight sailing and maneuverability are highly improved. For programming functions of the Roboat, the famous software: LabView is used to calculate algorithms for perfectly achieving the new missions of ONR's 8th International Roboat Competition. The overall Roboat system components is shown in Figure 1.



Figure 1 Diagram of overall Roboat system components



## 2. Mechanical and Electronic Systems

### 2.1. Ship Design

We use trimaran hull design for our Roboat this year, which is different from last year. We hope our Roboat to look like a real ship such as naval ship. After discussion, a triple-hull trimaran was adopted. We outlined the ship and designed the hull shape with Rhino software as shown in Figure 2. Thankfully, the Horizon which is a yacht company can help us to build the ship. Firstly, we went to the Horizon Company to make PVC board bond together, then imported Rhino drawing into CNC machine for processing. Finally, we processed on this untrimmed ship with grinding, cutting, and painting.

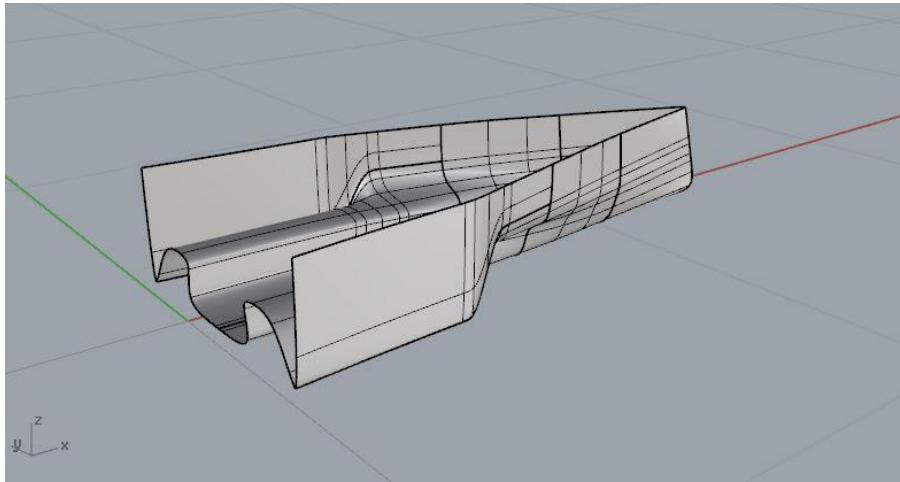


Figure 2 Ship hull design with Rhino software

## 3. Programming

### 3.1. Navigation

#### 3.1.1. Fuzzy Control

##### (i) Crisp Inputs and Outputs

The crisp input used in our unmanned surface vehicle is  $Error^\circ$ , which was presented in the previous chapter. The crisp outputs are the duty cycles that can control the DC brush (motors) thrusters. The Pulse Width Modulation (PWM) will be introduced before the discussion on duty cycles. PWM can be implemented by digital output devices. This technique can simulate the analog output by tuning the “high time” duration ( $t$ ) of a square wave. The ratio between high time duration ( $t$ ) and cycle time ( $T$ ) is known as the duty cycle, The equation of duty cycle is shown in Equation (3.8).

$$Dutycycle = \frac{t}{T} \quad (3.8)$$

## (ii) Membership Functions of Fuzzy Control

Managing the speed of the unmanned surface vehicle involves a twin-hull design, and its speed is less than 5 knots. This USV uses two thrusters, and the fuzzy controllers of these thrusters are designed separately. Equation (3.9) shows the membership functions of the input, and these functions can be tuned by adjusting for variables  $a$ ,  $b$ ,  $c$  and  $d$  in Equation (3.9). Equation (3.10) depicts the output membership functions as variables  $\alpha$ ,  $\beta$  and  $\gamma$  which represent duty cycles where a negative duty cycle value indicates that a thruster is in reverse.

In Equation (3.9), the variable  $x$  is the crisp input ( $Error^\circ$ ) while variable  $y$  in Equation (3.10) is the crisp output (duty cycle). The output membership functions are singleton membership functions. These functions are used due to the fact that very effective functional capabilities can be achieved with the fuzzy system only when singleton fuzzification is utilized .

$$\begin{aligned} \mu_{fuzzyIn1}(x) &= \begin{cases} 1 & (-180^\circ < x < a^\circ) \\ \frac{b-x}{b-a} & (a^\circ \leq x \leq b^\circ) \\ 0 & (b^\circ < x \leq 180^\circ) \end{cases} \\ \mu_{fuzzyIn2}(x) &= \begin{cases} 0 & (-180^\circ < x < a^\circ) \\ \frac{x-a}{b-a} & (a^\circ \leq x < b^\circ) \\ 1 & (b^\circ \leq x \leq c^\circ) \\ \frac{d-x}{d-c} & (c^\circ < x \leq d^\circ) \\ 0 & (d^\circ < x \leq 180^\circ) \end{cases} \\ \mu_{fuzzyIn3}(x) &= \begin{cases} 0 & (-180^\circ < x < c^\circ) \\ \frac{x-c}{d-c} & (c^\circ \leq x \leq d^\circ) \\ 1 & (d^\circ < x \leq 180^\circ) \end{cases} \end{aligned} \quad (3.9)$$

$$\begin{aligned} \mu_{fuzzyOut1}(y) &= \begin{cases} 1 & (y = \alpha) \\ 0 & (y \neq \alpha) \end{cases} \\ \mu_{fuzzyOut2}(y) &= \begin{cases} 1 & (y = \beta) \\ 0 & (y \neq \beta) \end{cases} \\ \mu_{fuzzyOut3}(y) &= \begin{cases} 1 & (y = \gamma) \\ 0 & (y \neq \gamma) \end{cases} \end{aligned} \quad (3.10)$$

Since two thrusters of the USV use the same input membership functions in this study, the output membership functions are separately designed. **錯誤! 找不到參照來源。** shows the input membership functions when variables  $[a,b,c,d]=[-50,-0.5,0.5,50]$  .  $\mu_{fuzzyOut2}(y)$  decides on the output values when  $b^\circ \leq Error^\circ \leq c^\circ$  because other membership functions are all equal to 0. In addition,  $\mu_{fuzzyOut2}(y)$  is determined by the variable  $\beta$ , which means that this variable affects

the amplitude of crisp outputs when  $b^\circ \leq Error^\circ \leq c^\circ$ . Taking the results from 錯誤! 找不到參照來源。 for example, the crisp output values (60% duty cycle) of the two thrusters are equal to the variable  $\beta$  when  $b^\circ \leq Error^\circ \leq c^\circ$  in Equation (3.10). Thus, the cruising speed is adjustable by tuning the variable  $\beta$ .

The variables  $b$  and  $c$  are determined by the precision of the electric compass. The accuracy of the electric compass we used is to 0.1 degrees; therefore, we used  $[b,c]=[-0.5,0.5]$  for our fuzzy control.

### 3.2. Obstacle avoidance

For this mission, first, in front of the entrance gate made of four buoys, we use web camera to capture the image message of the entrance gate and use our designed image recognition method to analyze the colors of the buoys and drive the propellers to force the Roboboat to approach the designated destination gate which is predefined by AUVSI. The radar will be used to detect the obstacles' distances and collision angles and these sensing messages will feedback to control the propellers to avoid hitting the buoys. Figure 3 is the flow chart for obstacle avoidance.

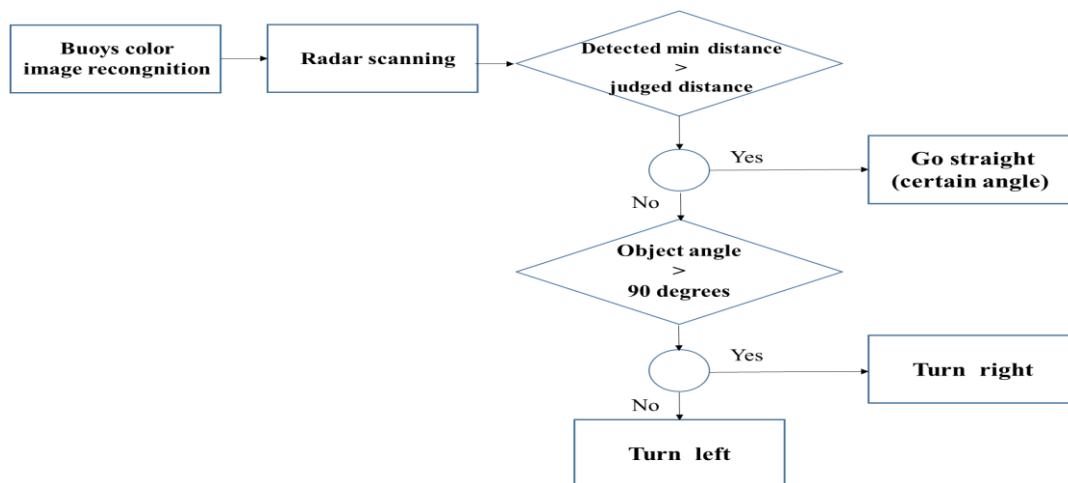


Figure 3 Flow chart of mission's program

#### 3.2.1. Radar

The following Table is the features of the used sensing radar with a type LMS 100.

##### (i) Operating principle of the SICK LMS100

The LMS100 is an electro-optical laser measurement system that electro-sensitively scans the perimeter of its surroundings in a plane with the aid of laser beams. The LMS100 measures its surroundings in two-dimensional polar coordinates. If a laser beam is incident to an object, the position is determined in the form of

distance and direction.

### 3.3. Automated docking

There are three main steps for achieving this mission: automated docking. First, the Roboboat would arrive at the specified waypoint by the propeller control System of the Roboboat. Second, the vision is captured by the USB Webcam, Logitech HD WebCam C525s, and then processed via LabView Vision Assistant which will display the results (judgment of the designated shape of dock by AUVSI) in every calculated step. Finally, the relative distance and desired turning angle between the Roboboat and target are calculated, and then Arduino board, Mega-2560 receives the delivering data pairs (relative distance and desired turning angle) to control the propeller of the Roboboat. Figure 4 is the block diagram of achieving the automated docking.

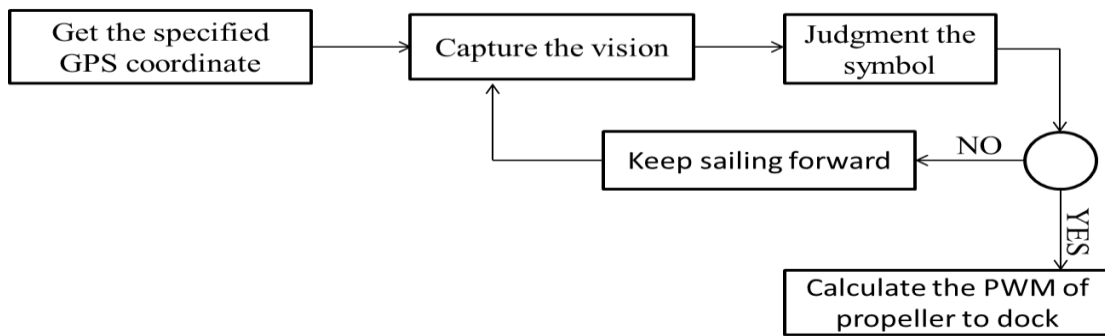


Figure 4 Flow chart of automated docking

#### 3.3.1. Identification of Symbols

##### Step 1: Color Threshold

The Color Threshold module is used to remove part of the image to fit the specified color range. There are three forms: HSL, HSV, RGB, can be chosen, each of them has an appropriate application environment based on the intensity of hue, saturation and luminance of the testing environment.

##### Step 2: Basic Morphology

The Morphology VI is used to perform morphology operations on the vision, and this operation should perform in binary image. The main functions of this module are touching the border of an image, removing noisy particles, and removing unwanted particles based on the user characteristics.

##### Step 3: Particle classification

Based on the specified application, a set of training samples that represent the properties of the entire population of samples wanted to be classified is labeled. The flow chart of this process is illustrated as Figure 5.



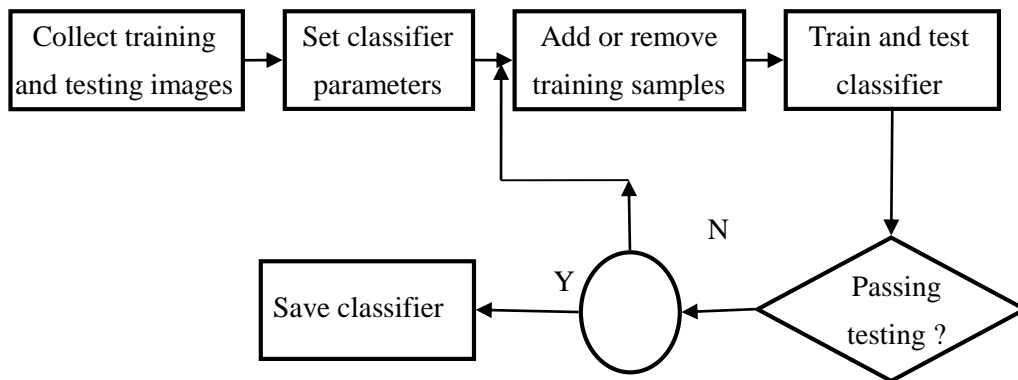


Figure 5 Flow chart of VIs process

### 3.4. Acoustic beacon positioning

For achieving the mission of precisely detecting the location of the voiced pinger, Roboboat is firstly guided by our deigned controller which is navigated by GPS to the waypoints where the position of mission arranged in priori. In this mission, the design objective is to detect the direction of an arranged pinger with a colored bouy which is set up under water. In order to identify the location of this pinger, we use a pair of hydrophones to receive the phase difference of incoming frequencies in different channels. Based on algorithms of beamforming Delay-and-Sum technique, we could get the direction and distance of voiced pinger, and then control the propeller of Roboboat to get there. When Roboboat arrives at the waypoint where the location of candidate pinger is, the webcam will capture the color of bouy, and WiFi is then used to send back to headquarter.

#### 3.4.1. Application of Devices

##### (i) Frequency Detecting Sensor

To detect the frequency of pinger under the water, the Brüel & Kjær Hydrophone Type 8103 which is with a small-size, high-sensitivity transducer for making absolute sound measurements over the frequency range 0.1Hz to 180 kHz are chosen. This sensor has a really high sensitivity relative to its size and good all-round characteristics which make it generally being applicable to laboratory, industrial and educational usage purpose. The 8103's high-frequency response is especially valuable when applying in acoustic investigations of marine animals and in the measurement of the pressure-distribution patterns in ultrasonic-cleaning baths.

##### (ii) Amplifier

We use B&K 2692 as the amplifier of hydrophone 8103, the output signal will be sent to the signal control board: arduino. The following points are the features of B&K

2692:

### (iii) MyRIO

To sample the high frequency pulse from pinger, we choose the portable reconfigurable I/O (RIO) device from National Instrument. The sampling frequency of myRIO is up to 500kHz, and it places dual-core ARM® Cortex™-A9 real-time processing. The features of myRIO let me can use it as a microcomputer, so that even this mission has a high frequency to sampling, it wouldn't make afford to mother board.

		
Figure 6 Hydrophone 8103	Figure 7 Amplifier 2692	Figure 8 MyRIO

### 3.4.2. Software Programming Process

The acoustic signal will be sampled and discretized by myRIO, and then we use a bandpass filter to remove the signals which are not emitted from pinger in the program. For dealing with this mission, Delay-and-Sum Technique which is introduced in the below section will be utilized to position the direction of pinger, and output the direction message for controlling the embedded propeller to the location of the pinger. Delay-and-Sum method is a common method on signal processing technique in sensor arrays for directional signal transmission, and can be used detect the direction and location of a sound resource (pinger) by time difference between two used water proof microphones and is easy to implement. For practical experiments, the number of hydrophones is higher, and the accuracy of direction of pinger can be obtained. However, we found that the limitation of myRIO is its count of time. For LabView, the count of time of device's detection need to be million second, then according to delay-and-sum method and the speed of water, the distance of two microphone must be more than 100m. However the width of boat is only 0.66m, the distance is obviously not enough for calculating delay-and-sum technique. Hence, we proposed a solution to this dilemma that using cross-correlation method to count how many samples delay, and the samples multiple with sampling time would be delay time. Using the pre-operated method to calculate the delay time won't limit by the count of time, so that the distance

of microphone could be 0.66m. The Figure 9 shows us the overall flow chart of acoustic beacon positioning method used in this investigation.

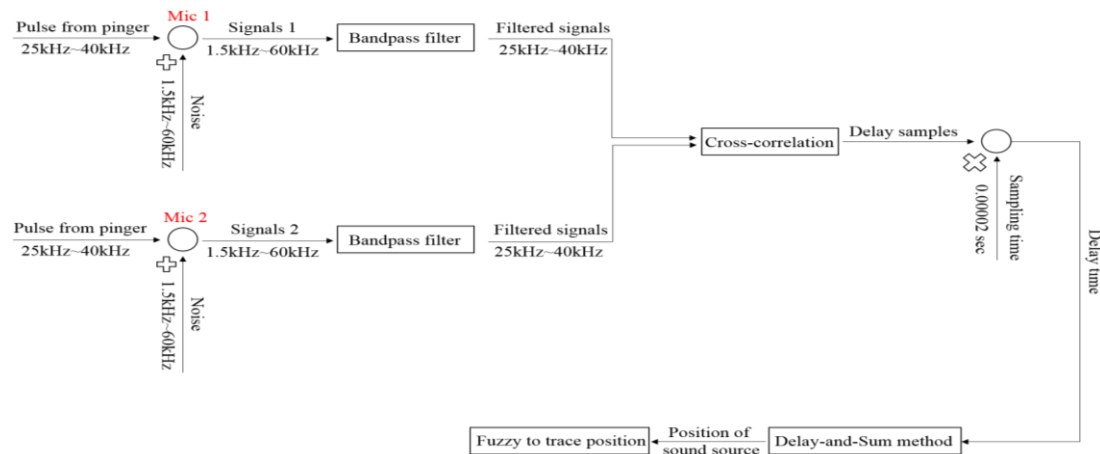


Figure 9 Flow chart of Acoustic beacon positioning

### 3.5. Interoperability challenge

The following Figures are the control process, simulation results, and practical tests for guiding the controlled Four-Rotor Rotorcraft to the desired waypoints. In Figure 10, the Earth-frame  $(X, Y, Z)$  and the Euler angles  $(\phi, \theta, \psi)$  are selected as state variables is to guide the controlled Four-Rotor rotorcraft to the predefined waypoints. In this control design, the environmental disturbance: wind effect is taken into consideration, and one nonlinear robust control is developed to deal with this disturbance corrupted tracking problem.

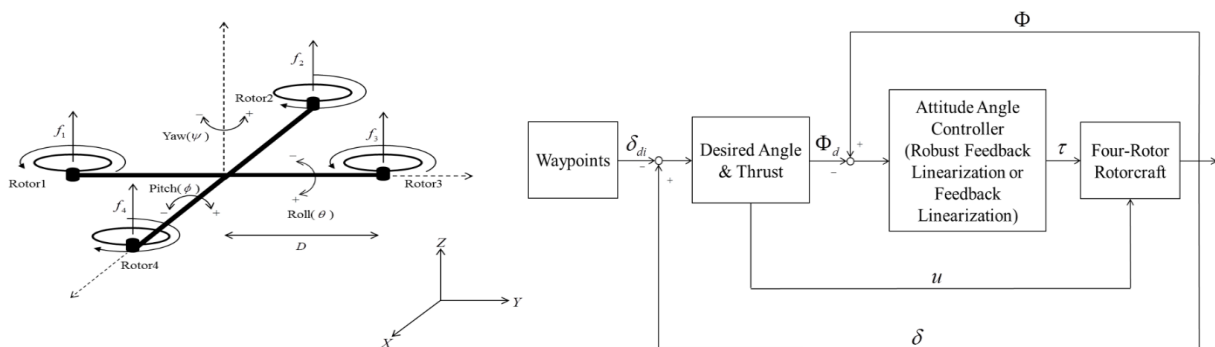


Figure 10 Coordinate definition of the controlled Four-Rotor Rotorcraft and control block diagram of Four-Rotor rotorcraft design process

### Simulation and Practical Results

An irregular tracking path with the combination of straight line and Zig-Zag pattern are arranged and the waypoints are arbitrarily chosen for verifying the control



performance of our proposed method is executed as below. From the above simulation results, the results reveal the fact that the Four-Rotor rotorcraft can precisely track the predefined waypoints

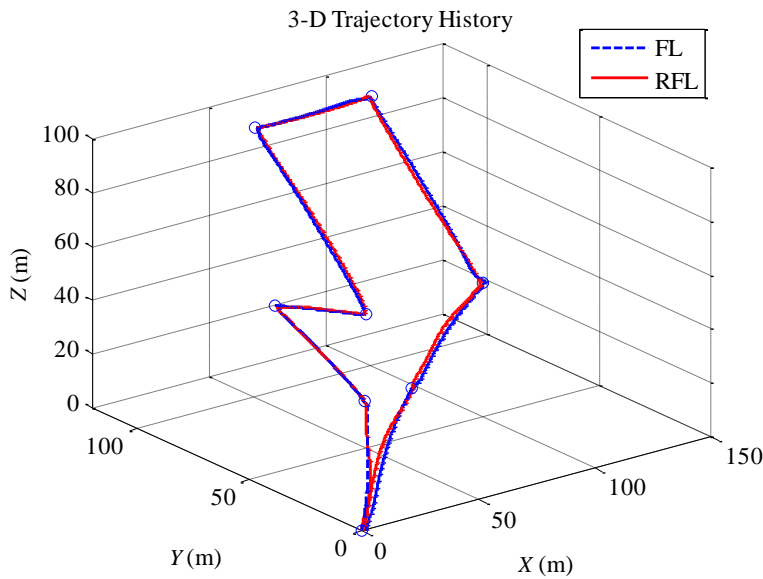


Figure 11 The 3-D flight trajectories of Four-Rotor rotorcraft (red-line and blue-line)

## 4. Reference

- [1] Davidson, K.S.M., and Schiff, L.I., "Turning and course keeping qualities of ships," *Trans. Soc. Nav. Archit. Mar. Eng.*, Vol. 54 (1946).
- [2] Vukic, Z. "Improving fault handling in marine vehicle course-keeping systems," *IEEE Proc. Robotics and Automation Magazine*, Vol.6, Issue 2, pp. 39 – 52 (1999).
- [3] Holzhter, T., "LQG approach for the high precision track control of ships," *IEEE Proc. Control Theory Appl.*, Vol. 144, Issue 2, pp. 121–127 (1997).
- [4] Fossen, *Guidance and Control of Ocean Vehicles*, John Wiley and Sons, New York, N.Y., pp. 19 (1994).
- [5] [http://zone.ni.com/reference/en-XX/help/372916L-01/nivisionconcepts/color\\_classification/](http://zone.ni.com/reference/en-XX/help/372916L-01/nivisionconcepts/color_classification/)
- [6] <http://www.bksv.com/doc/bp1702.pdf>
- [7] <http://www.bksv.com/products/transducers/conditioning/charge/2692a0i1?cmd=Description>
- [8] [http://www.sick-automation.ru/images/File/pdf/DIV05/LMS100\\_manual.pdf](http://www.sick-automation.ru/images/File/pdf/DIV05/LMS100_manual.pdf)
- [9] Jacob Benesty, Yiteng Huang, Jingdong Chen, "Microphone Array Signal Processing", Springer, Berlin Heidelberg, 2008

